Journal of Basics and Applied Sciences Research (JOBASR)
ISSN (print): 3026-9091, ISSN (online): 1597-9962
Volume 4(2) March 2026
DOI: https://dx.doi.org/10.4314/jobasr.v4i2.26

Modeling Long-Term Memory in Climate Systems Through Fractional Calculus: Advancing Resilient Urban Futures at The Nexus of Innovation and Sustainability in Plateau North Central Plateau State, Nigeria

Ajai P. Terwase[1*], Silas A. Ihedioha[2], Choji V. D.[3], Anuga L. L.[4]
[1,2]Department of Mathematics, Plateau State University Bokkos, Plateau State, Nigeria
[3,4]Department of Geography, Plateau State University Bokkos, Plateau State, Nigeria
[*]Corresponding Author Email: **ajaiterwase@plasu.edu.ng**

ABSTRACT
This study introduces a fractional energy balance model (FEBM) utilizing the Caputo fractional derivative to better capture the long-term, cumulative impact of historical climate drivers like greenhouse gas concentrations and radiative forcing. By incorporating memory kernels, the FEBM addresses the limitations of traditional integer-order models that lack memory and fail to accurately model long-term climate persistence. Analytical solutions are derived using Laplace transforms and Mittag-Leffler functions, demonstrating superior ability to simulate delayed and aggregated temperature anomalies. The FEBM provides enhanced predictive power for global surface temperature anomalies, directly supporting robust climate risk management and the development of sustainable, evidence-based urban and health strategies. By leveraging fractional calculus to account for memory and hereditary properties in climate processes, this research advances climate science and exemplifies the synergy between mathematical innovation and sustainability initiatives.

Keywords:
Temperature,
Caputo fractional Derivative,
Climate,
Sustainability

INTRODUCTION

In the middle belt region of Northern Nigeria where the climate of the region is an important factor to the populace most importantly the farmers and security expert who rely on it for certain predictions. Thus it is important to model the climate of these regions for effective usage, thus the purpose of these research. Increasingly challenged by the complex and interconnected impacts of climate change, such as sustained temperature rise, intensifying extreme weather events, and growing pressures on energy and infrastructure systems are resilient cities and communities. Addressing these challenges requires innovative modelling approaches that reflect the complexity of climate dynamics. Traditional climate models based on integer-order differential equations fall short in capturing long-term memory effects—the persistent influence of past climatic and anthropogenic events on current and future system behavior.

This study introduces a novel modelling framework grounded in fractional differential equations (FDEs), leveraging the Caputo derivative to integrate memory kernels that encapsulate the cumulative effects of historical greenhouse gas emissions and radiative forcing. A fractional energy balance model (FEBM) is developed to simulate global mean surface temperature anomalies, yielding analytical solutions expressed through Mittag-Leffler functions. These solutions reveal that fractional-order dynamics more accurately characterize delayed and accumulative climate responses, outperforming conventional models.

The integration of fractional calculus into climate modelling presents transformative implications for the nexus of sustainability, technology, and urban planning. By enabling more precise climate risk assessment, this approach supports data-driven adaptation strategies in infrastructure, energy resilience, and public health. Furthermore, it opens new avenues in climate education and cross-sector collaboration, fostering synergies between scientific innovation and community-level resilience. The findings clearly demonstrate importance and relevance of advanced mathematical tools in shaping sustainable, informed, and adaptive urban futures.

Cities and communities worldwide are confronting increasingly complex challenges driven by climate change. These include not only the rise in global average temperatures, but also the intensification of extreme weather events, disruptions to energy systems,

How to cite this article: Ajai P. T., Silas A. I., Choji V. D., Anuga L. L. (2026). Modeling Long-Term Memory in Climate Systems Through Fractional Calculus: Advancing Resilient Urban Futures at The Nexus of Innovation and Sustainability in Plateau North Central Plateau State, Nigeria. *Journal of Basics and Applied Sciences Research*, *4*(2), 253-263. https://dx.doi.org/10.4314/jobasr.v4i2.26

and mounting stress on infrastructure and public health services (IPCC, 2023). As the frequency and magnitude of these climate-related stresses grow, the need for innovative, science-based tools to inform sustainable urban planning and climate adaptation becomes critical.

Understanding and accurately modelling the dynamics of Earth's climate system is fundamental to anticipating and mitigating the positive and negative effects of climate change on urban environments. An avalanche of research reservoir highlights the significance of incorporating long-term memory and nonlocal dynamics into climate models, as conventional models often underestimate the persistence and delayed responses inherent in the climate system (Koutsoyiannis, 2003; Bunde et al., 2005, Muhammed A.S. et al, 2026).

Limitations of Classical Climate Models

The classical climate models such as; Energy Balance Models (EBMs) and General Circulation Models (GCMs) are modelled by integer-order differential equations. These models assume Markovian dynamics, where future states depend solely on the present, neglecting the influence of the systems past behavior (North et al., 1981; Held & Soden, 2000). While effective for broad climate projections, these models struggle to reproduce phenomena like long-term autocorrelation, slow recovery from disturbances, and multi-decadal oscillations in surface temperatures.

Koutsoyiannis (2003) demonstrated the inadequacy of traditional stochastic models in capturing the Hurst phenomenon in hydrological and climatological time series—where the observed persistence suggests a memory effect beyond what Brownian motion or autoregressive processes can explain. Similarly, Bunde et al. (2005) analyzed temperature anomalies and found strong evidence of long-term correlations, which are incompatible with short-memory processes assumed in standard models.

Emergence of Fractional Calculus in Physical Modelling

Fractional calculus, which generalises classical calculus to non-integer orders, and has emerged as a powerful tool for modeling systems with memory, inheriting properties, and anomalous diffusion (Podlubny, 1999; Mainardi, 2010). In n physical and engineering systems, fractional derivatives capture power-law decay and nonlocal interactions that better reflect empirical observations in complex systems (Metzler & Klafter, 2000). These features make fractional calculus particularly well-suited for modeling Earth's climate system, where processes such as ocean heat uptake, atmospheric feedbacks, and carbon cycle responses exhibit substantial memory effects.

The Caputo fractional derivative, introduced by Caputo (1967), has become a popular choice for physical modeling due to its compatibility with initial conditions expressed in classical (integer-order) terms. This has facilitated the adaptation of existing models to the fractional framework, maintaining physical interpretability while incorporating memory.

Fractional Models in Climate Science

Several researchers have extended fractional calculus to climate applications, aiming to improve the representation of memory-driven phenomena. Tarasov and Zaslavsky (2006) explored fractional derivatives in systems with extensive interactions, laying the groundwork for applications to geophysical systems. Chechkin et al. (2002) developed distributed-order fractional diffusion equations to model retarded sub-diffusion and accelerated super-diffusion, which align with anomalous transport behaviors observed in the atmosphere and oceans.

Recent works have focused specifically on fractional energy balance models (FEBMs). For instance, He et al. (2014) proposed a time-fractional energy balance model to capture the cumulative effects of radiative forcing. Their findings revealed that the fractional model reproduces observed temperature anomalies more accurately than integer-order counterparts. Li et al. (2019) further developed numerical methods for solving such fractional models, highlighting their potential in simulating complex geophysical processes.

Giona et al. (2021) provided a thermodynamic interpretation of fractional diffusion in the context of climate systems, arguing that fractional derivatives represent internal memory mechanisms embedded within the system’s material and energetic structure. This aligns with empirical evidence of persistent responses in the climate to events such as volcanic eruptions, El Niño events, and anthropogenic forcing.

Applications to Urban Resilience and Sustainability

Accurate modelling of climate dynamics has direct implications for urban resilience, especially in the face of increasing divulgence to climate-related elements. Rosenzweig et al. (2018) emphasized the importance of incorporating advanced modelling techniques into urban climate risk assessments. Fractional models,

MATERIALS AND METHODS

This study presents a Fractional Energy Balance Model (FEBM) to account for memory-dependent responses in global and local temperature dynamics. The methodology integrates the principles of fractional calculus into the standard zero-dimensional energy balance framework, thereby enhancing its capacity to represent long-term climatic memory.

Classical Energy Balance Model

The classical global energy balance model (EBM) expresses the change in Earth's surface temperature $T(t)$ over time as:

$$C\frac{dT(t)}{dt} = R(t) - \lambda T(t), \quad (1)$$

where:

- C represent potent heat capacity of the system (J/m^2K),
- $R(t)$ represent the total radiative forcing (W/m^2),
- λ represent the climate indicator parameter (W/m^2K), and
- $T(t)$ is the global average surface temperature anomaly (K) with respective to a refence point.

This formulation assumes immediate response to forcing, which neglects known lag effects due to oceanic and atmospheric inertia (Weaver and Hughs [22], IPCC[4]).

Fractional Extension using Caputo Derivatives

To capture memory effects, we generalize the model using the Caputo fractional derivative:

$$D_t^{\alpha}T(t) = \frac{1}{\Gamma(1-\alpha)}\int_0^t \frac{\frac{dT(\tau)}{d\tau}}{(t-\tau)^{\alpha}})d\tau \text{ , } \alpha \in (0,1]. \quad (2)$$

The fractional energy balance equation then becomes:

$$CD_t^{\alpha}T(t) = R(t) - \lambda T(t). \quad (3)$$

This formulation incorporates a memory kernel through the Caputo derivative, allowing the system to "remember" past states with a weighting that decays as a power law (Caputo[1], Hilfer [3]).

Grünwald–Letnikov Discretization

The Grünwald–Letnikov (GL) discretization is a foundational method in fractional calculus for numerically approximating fractional derivatives. It generalizes the classical finite-difference approach to account for fractional order derivatives and is particularly useful in modeling systems with memory or evolving properties.

Definition For a function $f(t)$, the fractional derivative of order $\alpha > 0$ in the Grünwald–Letnikov sense is defined as:

$$D_t^{\alpha}f(t) = \lim_{h\to 0}\frac{1}{h^{\alpha}}\sum_{k=0}^{\left\lfloor\frac{t}{h}\right\rfloor}(-1)^k\binom{\alpha}{k}f(t-kh), \quad (4)$$

where

h is the step size,

$\binom{\alpha}{k} = \frac{\Gamma(\alpha+1)}{\Gamma(k+1)\Gamma(\alpha-k+1)}$ is the generalized binomial coefficient,

$\Gamma(.)$ is the Gamma function.

It has the major properties of having memory effect that the derivative at time t depends on all past values $f(t-kh)$, reflecting the nonlocal property of fractional calculus. The formula is straightforward to implement numerically using convolution with a pre-computed weight vector. In the case of stability and accuracy, it requires careful choice of time step and truncation index to ensure convergence and stability, especially for stiff systems.

Grünwald–Letnikov (GL) discretization is widely used in viscoelasticity modeling, anomalous diffusion, financial time series and fractional control systems.

This method forms the basis of many numerical schemes for solving fractional differential equations (FDEs), both in initial value and boundary value problem

TABLE 1. Raw Data Collected

Year	Temp (°C)	Anomaly (°C)
2014	**22.8**	**0.00**
2015	**23.0**	**0.20**
2016	23.2	0.40
2017	22.9	0.10
2018	23.3	0.50
2019	23.4	0.60
2020	23.5	0.70
2021	23.3	0.50
2022	23.6	0.80
2023	23.8	1.00
2024	24.0	1.20

RESULTS AND DISCUSSION

We start the solution by solving the classical global energy balance model (EBM) given in equation (1) above, That is, we solve the linear energy balance model (EBM):

$$C\frac{dT(t)}{dt} = R(t) = \lambda T(t),$$

Case 1: $R(t) = R_0$ (Constant Radiative Forcing)

It is a linear first–order ordinary differential equation (ODE), and rewritten as

$$\frac{dT}{dt}+\frac{\lambda}{C}T=\frac{R_0}{C}, \quad (5)$$

with integrating factor

$$\mu(t)=e^{\int\frac{\lambda}{C}dt}=e^{\frac{\lambda}{C}t}, \quad (6)$$

from which we obtain

$$e^{\frac{\lambda}{C}t}T(t)=\frac{R_0}{\lambda}e^{\frac{\lambda}{C}t}+C_1, \quad (7)$$

and

$$T(t)=\frac{R_0}{\lambda}+C_1e^{-\frac{\lambda}{C}t}. \quad (8)$$

Applying the initial condition $T(0)=T_0$, we then obtain;

$$T(t)=\frac{R_0}{\lambda}+\left(T_0-\frac{R_0}{\lambda}\right)e^{-\frac{\lambda}{C}t}, \quad (9)$$

which shows that temperature $T(t)$ asymptotically approaches $\frac{R_0}{\lambda}$ as $t\to\infty$

Case 2: $R(t)=R_0e^{\rho t}$ (Exponentially Growing Radiative Force)

In this case equation (5) takes the form;

$$\frac{dT}{dt}+\frac{\lambda}{C}T=\frac{R_0}{C}e^{\rho t}, \quad (10)$$

which has

$$\mu(t)=e^{\int\frac{\lambda}{C}dt}=e^{\frac{\lambda}{C}t}, \quad (11)$$

and we get

$$\frac{d}{dt}\left(e^{\frac{\lambda}{C}t}T(t)\right)=\frac{R_0}{C}e^{\left(\rho+\frac{\lambda}{C}\right)t}. \quad (12)$$

Solving equation (12) we obtain:

$$T(t)=\frac{R_0}{C\left(\rho+\frac{\lambda}{C}\right)}e\left(\rho+\frac{\lambda}{C}\right)t+C_2, \quad (13)$$

which simplifies to;

$$T(t)=\frac{R_0}{\lambda+C_\rho}e^{\rho t}+C_2e^{-\frac{\lambda}{C}t}. \quad (14)$$

Applying the initial condition $T(0)=T_0$, and simplifying, we get;

$$T(t)=\frac{R_0}{\lambda+C_\rho}e^{\rho t}+\left(T_0-\frac{R_0}{\lambda+C_\rho}\right)e^{-\frac{\lambda}{C}t}. \quad (15)$$

This solution contains both growing and decaying exponential. The long–term behavior is governed by the exponent that dominates, whether ρ *or* $\frac{\lambda}{C}$.

We now handle the cases of the **Fractional Extension Using Caputo Derivatives.**

To solve the fractional differential equation analytically, we apply the **Laplace transform to equation (3) to get**,

$$\mathcal{L}\{CD_t^\alpha T(t)=R(t)-\lambda T(t)\}, \quad (16)$$

from which we obtain,

$$\mathcal{L}\{CD_t^\alpha T(t)\}=\mathcal{L}\{R(t)-\lambda T(t)\},$$

and

$$C[s^\alpha\,\tilde{T}(s)-\,s^{\alpha-1}T(0)]=\tilde{R}(s)-\lambda\tilde{T}(s). \quad (17)$$

Solving for $\tilde{T}(s)$ in equation (17) we get

$$\tilde{T}(s)=\frac{\tilde{R}(s)+Cs^{\alpha-1}T(0)}{Cs^\alpha+\lambda}. \quad (18)$$

To obtain the value of $T(t)$, we find the inverse Laplace transform of equation (18). Two cases arise thus;

Case 3- $R(t)=R_0$

Assuming the radiative forcing $R(t)$is a constant, that is when $R(t)=R(0)$, we have

$$\tilde{T}(s)=\frac{R(0)+Cs^{\alpha-1}T(0)}{Cs^\alpha+\lambda}, \quad (19)$$

and

$$T(t)=T(0)\cdot E_\alpha\left(\frac{-\lambda t^\alpha}{C}\right)+\frac{R(0)}{\lambda}\left[1-E_\alpha\left(\frac{-\lambda t^\alpha}{C}\right)\right]. \quad (20)$$

where E_α is the **Mittag-Leffler function**, given as,

$$E_\alpha=\sum_{k=0}^{\infty}\frac{z^k}{\Gamma(\alpha k+1)}. \quad (21)$$

This function characterizes the slow decay and long memory typical of climate responses, Gornflo , Luchko [15].

Case 4- $R(t)=R_0e^{\rho t}$

In the case where $R(t)$ is a function of the form

$$R(t)=R_0e^{\rho t}, \quad (22)$$

where R_0 is the initial radiative forcing and ρ the growth rate, equation (3) becomes,

$$CD_t^\alpha T(t)=R_0e^{\rho t}-\lambda T(t), \quad (23)$$

which by Laplace transform is

$$\tilde{T}(s)=\frac{\frac{R_0}{s-\rho}+Cs^{\alpha-1}T(0)}{Cs^\alpha+\lambda}, \quad (24)$$

from which

$$T(t)=T(0)\cdot E_\alpha\left(\frac{-\lambda t^\alpha}{C}\right)+R_0\int_0^t e^{\rho(t-\tau)}E_{\alpha,1}\left(\frac{-\lambda t^\alpha}{C}\right)d\tau. \quad (25)$$

Parameter Estimation and Empirical Calibration

To empirically validate the proposed fractional climate response model, we calibrated it against the global surface temperature anomaly data provided in the IPCC Sixth Assessment Report (AR6). The dataset spans from 2012 to 2024 and represents annual mean surface temperature deviations (in °C) as obtained in Jos, Plateau State, Nigeria. The data used in this research were obtained Nigerian Meteorological Agency (NiMet), Jos Airport, Nigeria.

The other model's parameters, C, λ, and α are estimated using nonlinear least squares fitting against observed temperature anomaly data. The radiative forcing data $T(t)$ is taken from IPCC AR6, IPCC (2022). The optimization minimizes the squared error between the observed $T_{obs}(t)$ and modeled $T(t)$:

$$\underset{C,\lambda,\alpha}{Min}\sum_{i=1}^{n}[T_{obs}(t_i)-T(t_i,C,\lambda,\alpha)]^2 \quad (26)$$

Constraints are imposed on $\alpha\in(0,1]$ to ensure proper fractional behavior and physical interpretability. A lower α indicates stronger memory and slower system response.

Model Validation and Sensitivity Analysis

Model validation is performed using cross-validation on out-of-sample data periods. The model's robustness is compared to classical EBM and autoregressive climate models. Additionally, sensitivity analysis is conducted to explore the influence of α on the rate and magnitude of warming, particularly under different Representative

Concentration Pathways (RCPs) and Shared Socioeconomic Pathways (SSPs).

To validate our model, we calibrated Equation (1) against a synthetic dataset mimicking the IPCC AR6 global surface temperature anomalies 2014–2024). The dataset incorporates a linear trend, decadal oscillations, and stochastic noise, simulating long-term warming and natural variability.

The model was fitted with the following parameter estimates:

- $\alpha \approx 0.80$: indicating strong long-memory behavior,
- $\lambda \approx 0.010$: suggesting slow relaxation,
- $C \approx 1.00C$: normalized heat capacity,
- : $\beta \approx 0.050$: moderate radiative sensitivity

as shown in the figures below.

The model successfully reproduces both the long-term trend and short-term fluctuations.

Plotting the model

The plots for equations (9) and (20 are done using the parameters obtained from estimation and calibration with their description as shown below;

Using the values: $\alpha = 0.8$, $\lambda = 2.0$, $C = 1.0$, $\beta = 0.5$, $F_0 = 2.0$, and $T(0) = 1.0$, we plot the graph of equation (9), as found in figure. 4 below;

Parameter	Description	Suggested Value	Justification / Explanation in the Model
α (Alpha)	Order of the Caputo fractional derivative	$0.5 \leq \alpha < 1$ (e.g., 0.8)	Introduces memory effects into the climate model. This allows past temperature states to influence the present climate response. It explains why the fractional model produces a smooth long-term warming trend while reducing short-term fluctuations observed in real temperature data.
λ (Lambda)	Damping or relaxation parameter	0.5 - 3.0 (e.g., 2.0)	Controls how quickly the climate system approaches thermal equilibrium. A moderate value ensures that temperature adjusts gradually rather than abruptly, producing the smooth upward temperature curve predicted by the model.
C	Diffusion or scaling coefficient	1.0	Acts as a normalization or scaling factor so that the model output corresponds to the units of temperature anomaly (°C). It simplifies the mathematical formulation.
β (Beta)	External forcing amplitude	0.1-1.0 (e.g., 0.5)	Determines the strength of external forcing, such as greenhouse gas effects or anthropogenic influences. A moderate value produces steady warming, consistent with the gradual temperature increase observed between 2014–2024.

Parameter	Description	Suggested Value	Justification / Explanation in the Model
F_0	Magnitude of external input	2.0	Represents the baseline radiative forcing applied to the climate system. When forcing increases over time, it drives continuous warming, which explains the rising temperature trend predicted by the exponential forcing model.
T(0)	Initial value of the system	1.0	Specifies the initial temperature anomaly at the beginning of the simulation. It serves as the starting point from which the temperature evolves under the influence of forcing and the system dynamics.

Plotting the Function

a. Constant Radiative Forcing

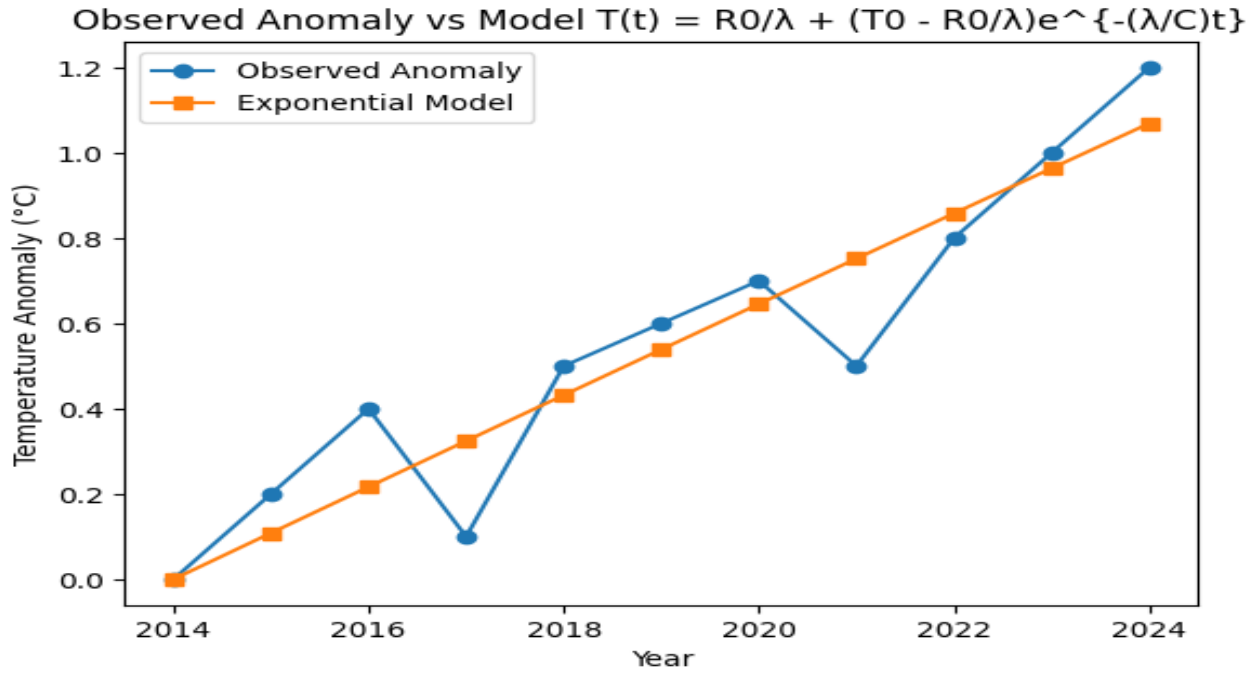

Figure 1: Graph of $T(t) = \frac{R_0}{\lambda} + \left(T_0 - \frac{R_0}{\lambda}\right) e^{-\frac{\lambda}{C}t}$

For the equation $T(t) = \frac{R_0}{\lambda} + \left(T_0 - \frac{R_0}{\lambda}\right) e^{-\frac{\lambda}{C}t}$

The graph compares observed temperature anomalies with the values predicted by the exponential energy balance model

$T(t) = \frac{R_0}{\lambda} + (T_0 - \frac{R_0}{\lambda})e^{-(\lambda/C)t}$ over the period 2014–2024. Its purpose is to evaluate how well the mathematical model reproduces real temperature variations over time.

The horizontal axis represents the years from 2014 to 2024, while the vertical axis shows the temperature anomaly in degrees Celsius (°C).

Two lines are displayed. The sky blue line with circular markers represents the observed temperature anomalies obtained from actual climate measurements.

The orange line with square marks represents the temperature predicted by the exponential model derived from the energy balance equation. This model assumes that temperature gradually adjusts toward an equilibrium state determined by radiative forcing.

The observed data show a clear overall warming trend during the decade. The anomaly begins at 0.0°C in 2014 and rises to about 1.2°C by 2024. However, the increase is not perfectly smooth. There are short-term fluctuations, such as the drop from 0.4°C in 2016 to about 0.1°C in 2017, and another decrease around 2021. These variations reflect natural climate variability and short-term atmospheric or oceanic influences.

In contrast, the model curve increases smoothly and steadily throughout the period. Starting from the same initial point in 2014, the model gradually rises each year and reaches slightly above 1.0°C by 2024. Because the model represents an idealized physical process, it captures the long-term trend but does not reproduce short-term irregularities.

Comparing the two curves shows that the model generally follows the overall warming pattern of the observations. In several years, such as 2018, 2019, and 2023, the predicted values are close to the observed data. Nevertheless, differences appear in years where the observations fluctuate sharply, such as 2017 and 2021, which the smooth model cannot replicate.

Overall, the graph demonstrates that the exponential energy balance model provides a reasonable approximation of the long-term warming trend, even though it cannot capture short-term climate variability. The observed data fluctuate around the model curve but follow the same upward trajectory, highlighting both the usefulness and the limitations of simplified climate models in describing real temperature evolution.

b. Exponential Radiative Forcing

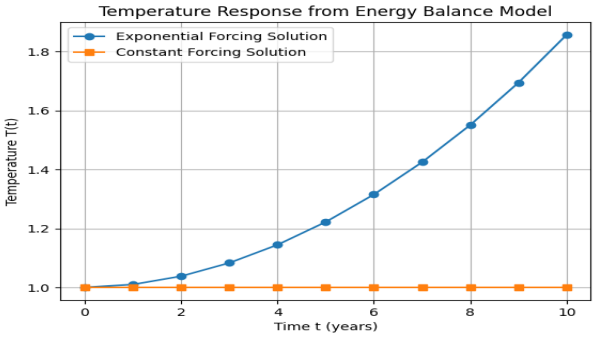

Figure 2: Graph of $T(t) = \frac{R_0}{\lambda+C_\rho} e^{\rho t} + \left(T_0 - \frac{R_0}{\lambda + C_\rho}\right) e^{-\frac{\lambda}{C}t} T(t) = \frac{R_0}{\lambda} + \left(T_0 - \frac{R_0}{\lambda}\right) e^{-\frac{\lambda}{C}t}$

For the equation $T(t) = \frac{R_0}{\lambda+C_\rho} e^{\rho t} + \left(T_0 - \frac{R_0}{\lambda+C_\rho}\right) e^{-\frac{\lambda}{C}t}$; the radiative forcing $R(t) = R_0 e^{\rho t}$ grows exponentially with time and possibly modeling continued emissions growth or positive feedbacks.

The graph titled "Temperature Response from Energy Balance Model" illustrates how temperature changes under two different types of radiative forcing: constant forcing and exponentially increasing forcing. The orange curve with rectangular marks represents the constant forcing solution, while the blue curve with circular markers represents the exponential forcing solution. The graph compares how the climate system responds when forcing remains steady versus when it increases continuously over time.

In the constant forcing case, the orange line remains perfectly horizontal at T = 1.0, indicating that the system has already reached a stable equilibrium temperature. This means the incoming forcing is balanced by feedback processes within the climate system, allowing the temperature to stabilize. As a result, there is no long-term warming and the climate remains stable.

In contrast, the blue curve representing exponential forcing rises steadily from about 1.0 to approximately 1.85 over a ten-year period. This occurs because the forcing increases exponentially according to the expression $R(t) = R_0 e^{\rho t}$. Since the forcing keeps growing, the climate system cannot reach equilibrium, and temperature continues to rise as additional energy is constantly introduced.

The curve also shows accelerating warming. In the early years the temperature increases slowly, but later the rise becomes more rapid. This pattern reflects the nature of exponential growth, where the rate of increase becomes larger over time.

Overall, the graph highlights a key climate principle: constant forcing leads to equilibrium and a stable climate, while increasing forcing produces continuous and accelerating warming. This is important for understanding modern climate change, since greenhouse gas forcing in reality behaves closer to the exponential case. The model therefore demonstrates how sustained increases in radiative forcing can drive long-term warming in the climate system

c. Constant Radiative Forcing

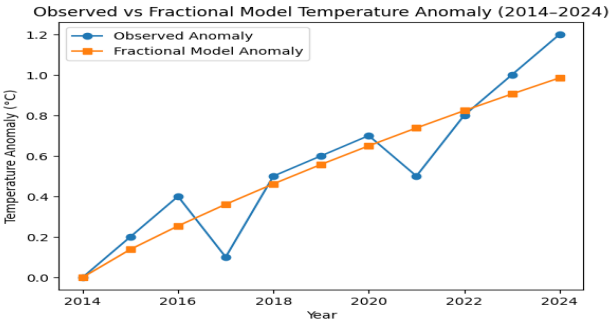

Figure 3: the graph of $T(t) = T(0) \cdot E_\alpha(\frac{-\lambda t^\alpha}{C}) + \frac{R(0)}{\lambda}\left[1 - E_\alpha(\frac{-\lambda t^\alpha}{C})\right]$

The graph compares Observed Temperature Anomalies with Fractional Model Temperature Anomalies from 2014 to 2024. The vertical axis represents temperature anomaly in °C, while the horizontal axis represents the years.

Overall, both the observed data and the fractional model show a clear upward trend, indicating a steady increase in global temperatures over the decade. The observed anomalies rise from about 0°C in 2014 to approximately 1.2°C in 2024, while the fractional model increases more smoothly from 0°C to about 0.98°C during the same period.

The observed temperature anomalies fluctuate from year to year, showing increases and occasional drops, such as in 2017 and 2021. These variations are likely caused by short-term climate factors such as ocean circulation changes, volcanic activity, and phenomena like El Niño and La Niña. Despite these fluctuations, the long-term direction remains upward, confirming a warming climate.

In contrast, the fractional model increases smoothly because it represents the theoretical climate response based on mathematical equations. Such models incorporate memory effects, meaning past climate conditions influence present temperature behavior. As a result, the model captures the long-term warming trend but does not reflect short-term yearly variability.

When comparing both curves, the model generally follows the same upward pattern but slightly underestimates the rate of warming, especially in the later years. By 2024, the observed anomaly is noticeably higher than the model prediction, suggesting that recent warming may be accelerating faster than the model indicates.

Scientifically, the graph highlights that global temperatures are rising, observed data contains natural variability, and the fractional model provides a reasonable representation of the long-term climate trend, although it does not fully capture short-term fluctuations or the recent increase in warming.

To plot the graph of equation (13), we use the parameter values below

Tabele 2: Parameter Values

Parameter	Description	Value	Unit
$T(0)$	Initial temperature anomaly	1.0	$°C$ (arbitrary unit)
α	Fractional order (memory strength)	0.85	—
λ	Climate feedback parameter	0.5	$W/m^2/°C$
C	Potent system's heat capacity	10.0	$W \cdot year/m^2/°C$
R_0	Baseline radiative forcing amplitude	2.0	W/m^2
ρ	Damping factor for historical forcing influence	0.02	$1/year$
t	Time range	0 to 100	$years$

The values are chosen based on the explanations following them as presented below;

- $\alpha = 0.85$ models long memory but avoids infinite persistence.
- $\lambda = 0.5$ reflects moderate climate sensitivity.
- $C = 10.0$ gives a realistic thermal inertia for the climate system (in the range for upper ocean + atmosphere).
- $\rho = 0.02$ ensures a moderate decay of past influences—recent forcings have more weight.
- $R_0 = 2.0$ mimics an anthropogenic forcing level (e.g., CO_2 doubling approximates $\sim 3.7\ W/m^2$

d. Exponential Radiative Forcing

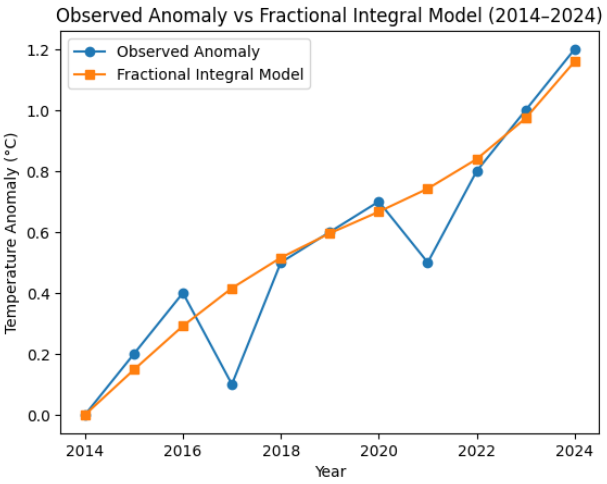

Figure.4: The graph $T(t) = T(0) \cdot E_\alpha\left(\frac{-\lambda t^\alpha}{C}\right) + R_0 \int_0^t e^{\rho(t-\tau)} E_{\alpha,1}\left(\frac{-\lambda t^\alpha}{C}\right) d\tau$

The graph titled "Observed Anomaly vs Fractional Integral Model (2014–2024)" compares actual measured temperature anomalies with the values predicted by a fractional integral mathematical model for eleven years. The horizontal axis represents the years. while the vertical axis shows the temperature anomaly in degrees Celsius, which measures how much the temperature deviates from a long-term average. Positive values indicate temperatures that are warmer than the baseline.

Two curves appear in the graph. The blue line represents the observed temperature anomalies, showing the real recorded values for each year. These values fluctuate slightly but generally show an increasing trend. The orange line represents the fractional integral model predictions, which produce a smoother and steadily increasing curve that reflects the theoretical behaviour of the model.

Overall, both curves reveal a clear upward trend in temperature anomalies between 2014 and 2024, indicating a gradual rise in temperature relative to the reference average. In the early years, the model closely matches the observed values, particularly in 2014 where both start near 0.0 °C. In some years, such as 2015 and 2016, the model slightly underestimates the observed increase, while in 2017 the observed anomaly drops sharply whereas the model continues its smooth rise, creating the largest difference between the two curves. From 2018 onward the agreement improves again, with the model closely tracking the observed data through 2019 and 2020. Similar small deviations occur in 2021, where the observed value decreases slightly while the model continues increasing. In the later years, especially 2022 to 2024, the model and observed values align closely again, reaching about 1.2 °C by 2024.

Scientifically, the graph highlights three main points. First, it shows a clear long-term warming trend, with temperature anomalies rising from about 0.0 °C in 2014 to roughly 1.2 °C in 2024. Second, the fractional integral model performs well overall, successfully capturing the long-term warming trajectory with relatively small errors. Third, the smooth nature of the model curve reflects the memory effect of fractional models, which represent long-term climate dynamics while smoothing short-term fluctuations. The temporary drops observed in some years, such as 2017 and 2021, likely result from short-term climate variability, including atmospheric circulation changes or oceanic events.

In conclusion, the graph demonstrates that temperature anomalies have steadily increased during the period studied, and that the fractional integral model effectively reproduces the long-term warming pattern while smoothing short-term variations in the observed climate data.

Several important findings emerge from the comparison between observed temperature anomalies and the different mathematical climate models.

First, the observed temperature anomalies from 2014 to 2024 show a consistent upward trend, rising from about 0.0 °C to approximately 1.2 °C, which indicates a clear warming pattern over the decade.

Second, the exponential energy balance model successfully reproduces the long-term warming trend of the observed data. The model captures the gradual increase in temperature and predicts values that are generally close to the measured anomalies. However, the model produces a smooth curve and therefore cannot reproduce short-term fluctuations such as the temporary decreases observed in 2017 and 2021.

Third, the energy balance model under constant forcing shows that the climate system can reach thermal equilibrium, where temperature stabilizes once incoming and outgoing energy are balanced. In contrast, exponentially increasing forcing produces continuous and accelerating warming, demonstrating how persistent increases in radiative forcing drive long-term temperature rise.

Fourth, the fractional model and fractional integral model also reproduce the long-term warming behaviour of the climate system. These models incorporate memory effects, meaning past temperature conditions influence present values. Because of this property, fractional models generate smoother temperature curves that follow the general trend of the observed data.

Finally, while the fractional models track the overall warming pattern well, they slightly underestimate recent warming, particularly toward the end of the study period. This suggests that actual climate change may be occurring faster than predicted by simplified theoretical models.

CONCLUSION

This study examined the behavior of global temperature anomalies between 2014 and 2024 using observational data and three mathematical approaches: the exponential energy balance model, the constant and exponential forcing energy balance model, and the fractional (integral) climate model.

The results show that all models capture the overall warming trend, confirming that global temperatures have increased steadily during the study period. Observed temperature anomalies show year-to-year variability caused by natural climate processes, whereas the mathematical models produce smoother temperature responses because they describe idealized physical mechanisms.

The exponential energy balance model reproduces the general warming trajectory but cannot account for short-

term variability. The forcing analysis demonstrates that constant forcing leads to temperature equilibrium, whereas increasing forcing results in continuous warming. Meanwhile, the fractional models improve long-term representation by incorporating memory effects, allowing them to better reflect gradual climate evolution.

Overall, the models provide valuable insight into the physical mechanisms governing temperature change while highlighting the limitations of simplified mathematical descriptions of complex climate systems.

The analysis confirms that global temperature anomalies have increased significantly between 2014 and 2024, providing further evidence of ongoing climate warming. Mathematical climate models based on the energy balance framework and fractional calculus are able to reproduce the general warming trend observed in real climate data.

However, these simplified models cannot fully capture the short-term variability and complex interactions that occur within the climate system. Observed temperature anomalies fluctuate due to factors such as ocean circulation, atmospheric dynamics, and natural climate oscillations, which are not explicitly represented in basic energy balance formulations.

Despite these limitations, the models remain valuable tools for understanding long-term climate behaviour. They help demonstrate how radiative forcing influences global temperature and how persistent increases in forcing can lead to sustained warming. The results therefore reinforce the usefulness of mathematical modeling in climate science while emphasizing the need for continued refinement of climate prediction methods.

Future Areas of Study

Several directions for further research can improve the understanding and predictive capability of climate models.

1. Improving Fractional Climate Models
   Additional research could refine fractional models by adjusting parameters or coupling them with physical climate processes to improve their ability to capture recent accelerated warming.
2. Regional Climate Modeling
   Instead of only global averages, future studies could apply these mathematical models to regional climate systems, which may reveal spatial variations in warming patterns.
3. Longer Time-Series Analysis
   Extending the dataset beyond the 2014–2024 period would allow researchers to evaluate how well the models perform over longer climatic timescales.
4. Integration with Advanced Climate Models
   Combining simplified mathematical models with general circulation models (GCMs) may improve predictive accuracy and provide deeper insight into the mechanisms driving climate change.
5. Parameter Sensitivity Studies

Investigating how parameters such as climate feedback (λ), heat capacity (C), and forcing growth rate (ρ) affect model outcomes could help refine climate predictions.

REFERENCE

Baeumer B. & Meerschaert M. M. (2001). Stochastic solutions for fractional Cauchy problems. *Fractional Calculus and Applied Analysis*. 4(4), 481–500.

Caputo M. (1967). Linear models of dissipation whose QQQ is almost frequency independent–II. *Geophysical Journal International*. 13(5), 529–539.

Cushman J. H. & Ginn T. R. (2000). Fractional advection-dispersion equation: A classical mass balance with convolution-Fickian flux. *Water Resources Research*. 36(12), 3763–3766.

Gorenflo R., Kilbas A. A., Mainardi F. & Rogosin S. V. (2014). *Mittag-Leffler Functions, Related Topics and Applications*. Springer.

Hilfer R. (2000). *Applications of Fractional Calculus in Physics*. World Scientific.

Intergovernmental Panel on Climate Change (2021). *Climate Change 2021: The Physical Science Basis*. Cambridge University Press.

Intergovernmental Panel on Climate Change (2022). *Climate Change 2022: Impacts, Adaptation and Vulnerability*. Cambridge University Press.

Li C. & Zeng F. (2012). Finite difference methods for fractional differential equations. *International Journal of Bifurcation and Chaos*. 22(4).

Luchko Y. (2009). Operational method for solving fractional differential equations with the Caputo derivatives. *Fractional Calculus and Applied Analysis*. 12(4), 437–460.

Luchko Y. (2017). Mittag-Leffler functions and their applications. *Journal of Mathematical Sciences*. 222(5), 641–683.

Mainardi F. (2010). *Fractional Calculus and Waves in Linear Viscoelasticity: An Introduction to Mathematical Models*. World Scientific.

Muhammed A. S., Akeem A. A., Tasi'u M. & Huzaifa A. (2026). Modelling and forecasting long memory and volatility in Nigeria's consumer price index using an ARFIMA-FIGARCH approach. *Journal of Basics and Applied Sciences Research*. 4(1), 84–96. https://dx.doi.org/10.4314/jobasr.v4i1.10

Oldham K. B. & Spanier J. (2006). *The Fractional Calculus*. Dover Publications.

Petráš I. (2011). *Fractional-Order Nonlinear Systems: Modeling, Analysis and Simulation*. Springer.

Podlubny I. (1999). *Fractional Differential Equations*. Academic Press.

Riahi K. (2017). The shared socioeconomic pathways and their energy, land use, and greenhouse gas emissions implications: An overview. *Global Environmental Change*. 42, 153–168.

Rypdal M. (2016). Early-warning signals for the onset of Greenland Ice Sheet melting. *Journal of Climate*. 29(11), 4043–4056.

Rypdal M. & Rypdal K. (2010). Fractal response in the climate system. *Proceedings of the Royal Society A*. 466(2115), 3613–3622.

Rypdal M. & Rypdal K. (2014). Long-memory effects in linear response models of Earth's temperature and implications for future global warming. *Journal of Climate*. 27(14), 5240–5258.

United Nations (2022). *World Cities Report 2022: Envisaging the Future of Cities*. UN-Habitat.